Millimetre Wave RADAR Spectra Simulation and Interpretation for Outdoor SLAM

Ebi Jose, Martin D. Adams
School of Electrical and Electronic Engineering,
Nanyang Technological University, Nanyang Avenue 639798, Singapore.
Email : ebi@pmail.ntu.edu.sg, eadams@ntu.edu.sg

***Abstract*— Millimetre Wave RADARs are more robust than most other sensors used in outdoor autonomous navigation in that their performance is less affected by dust, fog, moderate rain or snow and ambient lighting conditions.**

This paper describes a method to accurately simulate the range spectra using the RADAR range equation. This is very important in robot navigation (eg. SLAM) for generating predictions of what can be observed from different sensor locations and correspondingly, providing an interpretation for observed targets. To understand the MMW RADAR range spectrum and to simulate it accurately, it is necessary to know the noise distributions in the RADAR spectrum. A detailed noise analysis during signal absence and presence is carried out which shows various sources of noise affecting MMW RADARs. RADAR range bins are then simulated using the RADAR range equation and the noise statistics and are compared with real results in controlled environments. It will be demonstrated that it is possible to provide realistic predicted RADAR power/range spectra, for multiple targets down range.

Feature detection from the RADAR spectra based on target presence probability is then explained. The detection technique uses binary hypothesis testing. Results are shown comparing a new probability based feature detection with other standard feature extraction techniques such as constant threshold on raw RADAR data and Constant False Alarm Rate (CFAR) techniques. The results show that the proposed algorithm is more robust compared to other detection techniques as it does not require human assistance. This work is a step towards robust outdoor SLAM with MMW RADAR based continuous power spectra.

***Index Terms* - MMW RADAR, noise statistics, range estimation, Constant False Alarm Rate, target presence probability.**

I. Introduction

Current research on Simultaneous Localisation and Mapping (SLAM) focuses on mining, planetary-explorations, fire emergencies, battlefield operations as well as on agricultural areas. MMW RADAR provides consistent and fairly accurate range measurements for the environmental imaging required to perform SLAM in dusty, foggy and poorly illuminated environments [1]. Millimetre wave RADAR signals have the ability to penetrate many objects and can provide information of distributed targets that appear in a single observation. This work is conducted with a 77 GHz Frequency Modulated Continuous Wave (FMCW) RADAR which operates in the millimetre wave region of the Electro-Magnetic Spectrum.

For Localisation and Map building, it is necessary to predict the target locations accurately given a prediction of the vehicle/RADAR location. A method for accurately predicting the power-range spectra (or range bins) using the RADAR range equation and the knowledge of the noise distributions in the RADAR is explained in this paper.

Predicted observations are formed using this predicted state and the given RADAR equation, system and noise analyses to construct "predicted range-bins". The actual observations take the form of received power/range readings from the RADAR.

Section II briefly summarises related work, while section III describes FMCW RADAR operation and the noise affecting the range spectra. Section IV describes how power-range spectra can be simulated (predicted observations). This utilises the RADAR range equation and a noise analysis which considers the propagation of noise from its source in the receiver through the RADAR electronics to the final range output. Methods for estimating the true range from power-range spectra are given in section IV where a new robust range estimation technique based on target presence probability is presented. Section VI shows that the proposed algorithm is more robust compared to other detection techniques such as constant threshold on the power spectra and Constant False Alarm Rate (CFAR) methods as it does not require human assistance.

II. Related Work

In recent years RADAR for automotive purposes has gained interest in shorter range (< 200) metres applications. Most of the work in short range RADAR has focused on millimetre waves as this allows narrow beam shaping, which is necessary for higher angular resolution.

Steve Clark [2] presented a method for fusing RADAR readings from different vehicle locations into a two dimensional representation. The method selects one range point per RADAR observation at a particular bearing angle based on a certain received signal power threshold level. This method takes only one range reading per bin which is the nearest power return to exceed that threshold to the RADAR, discarding all others. In [3] Clark shows a millimetre wave RADAR based navigation system which utilises artificial beacons for localisation and an extended Kalman filter for fusing multiple observations. Human intervention is required for adjusting the threshold as the returned signal power depends on various object's RADAR Cross Section (RCS).

Boehmke *et al.* [4] succeed in producing three-dimensional terrain maps using a pulsed RADAR with a narrow beam

and high sampling rate. The work by Boehmke *et al.* was more concentrated on building a pulsed RADAR rather than RADAR data interpretation. The pulsed RADAR cannot give information on distributed or multiple targets.

Foessel shows the usefulness of evidence grids for integrating uncertain and noisy sensor information [5]. In [6], Foessel *et al.* show the development of a RADAR sensor model for certainty grids and also demonstrates the integration of RADAR observations for building three-dimensional outdoor maps. Certainty grids divide the area of interest into cells, where each cell stores a probabilistic estimate of its state [7] [8]. The proposed three-dimensional model by Foessel *et al.* has shortcomings such as the necessity of rigorous probabilistic formulation and difficulties in representing dependencies due to occlusion.

III. FMCW RADAR Operation and Range Noise

This section gives a brief introduction about the RADAR sensor and the Frequency Modulated Continuous Wave technique for obtaining target range. This is necessary for RADAR signal interpretation and for understanding and quantifying the noise in the power/range estimates. The RADAR is a 77 GHz frequency modulated continuous wave (FMCW) system. The transmitted power is 15 dBm and the swept band-width is 600 MHz. Figure 1 shows a schematic block diagram of an FMCW RADAR transceiver. In figure 1, input voltage to the Voltage Control Oscillator (VCO) is a ramp signal. The VCO generates a signal of linearly increasing frequency δf in the frequency sweep period T_d. This linearly increasing chirp signal is transmitted via the antenna. An FMCW RADAR measures the distance to an object by mixing received signals with a portion of the transmitted signal.

Let the transmitted signal $v_T(t)$ as a function of time, t be represented as

$$\begin{aligned} v_T(t) &= \mathrm{A}_T \cos\left[\omega_c t + \mathrm{A}_b \int_0^t t\,dt\right] + n_T(t) \\ &= \mathrm{A}_T \cos\left[\omega_c t + \frac{\mathrm{A}_b}{2} t^2\right] + n_T(t) \end{aligned} \tag{1}$$

where A_T is the amplitude of the carrier signal; ω_c is the carrier frequency (*i.e* 77 GHz); A_b is the amplitude of the modulating signal and $n_T(t)$ is a noise process present in the transmitting signal. The noise occurs inside the transmitting electronic sections.

At any instant of time, the received echo signal is shifted in frequency from the transmitted signal by a round trip time, τ. The received signal is

$$v_R(t-\tau) = \mathrm{A}_R \cos\left[\omega_c(t-\tau) + \frac{\mathrm{A}_b}{2}(t-\tau)^2\right] + n_R(t) \tag{2}$$

where A_R is the received signal amplitude and $n_R(t)$ is the noise component in the received signal. The sources of noise are external to the system (e.g., atmospheric noise, man-made interference) or internally produced at the receiver antenna and amplifies in the system. The internal noise present in both transmitted and received signals arises from spontaneous fluctuations of current or voltage in the electrical circuits [9].

In the mixer the received signal is mixed with a portion of the transmitted signal with an analog multiplier:

$$\begin{aligned} v_R(t-\tau)\, v_T(t) = \mathrm{A}_R\, \mathrm{A}_T &\left\{\cos\left[\omega_c t + \frac{\mathrm{A}_b}{2} t^2\right] + n_T(t)\right\} \\ &\left\{\cos\left[\omega_c(t-\tau) + \frac{\mathrm{A}_b}{2}(t-\tau)^2\right] + n_R(t)\right\} \end{aligned} \tag{3}$$

The output of the mixer, $v_{out}(t)$ is (using the trigonometric identity for the product of two sine waves: $\cos \mathrm{A}\ \cos \mathrm{B} = 0.5[\cos(\mathrm{A}+\mathrm{B}) + \cos(\mathrm{A}-\mathrm{B})]$)

$$\begin{aligned} v_{out}(t) = \frac{\mathrm{A}_R \mathrm{A}_T}{2}[\mathrm{B}_1 + \mathrm{B}_2] &+ \mathrm{A}_R \mathrm{A}_T \cos\left[\omega_c t + \frac{\mathrm{A}_b}{2} t^2\right] n_R(t) \\ &+ \mathrm{A}_R\, \mathrm{A}_T \cos\left[\omega_c(t-\tau) + \frac{\mathrm{A}_b}{2}(t-\tau^2)\right] n_T(t) \\ &+ \mathrm{A}_R\, \mathrm{A}_T n_R(t)\, n_T(t) \end{aligned} \tag{4}$$

where $\mathrm{B}_1 = \cos\left[(2\omega_c - \mathrm{A}_b\tau)\, t + \mathrm{A}_b t^2 + \left(\frac{\mathrm{A}_b}{2}\tau^2 - \omega_c \tau\right)\right]$ and $\mathrm{B}_2 = \cos\left[\mathrm{A}_b\, \tau\, t + \left(\omega_c\, \tau - \frac{\mathrm{A}_b}{2}\, \tau^2\right)\right]$

The second cosine term, B_2 corresponds to the beat frequency. The output of the IF filter consists of the beat frequency component, B_2 and the noise component while other components are filtered out. The beat frequency signal, f_b is directly proportional to the delay time, τ which is directly proportional to the round trip time to the target. The relationship between beat frequency and target distance is

$$\mathrm{R} = \frac{c\,\mathrm{T}_s}{2} \frac{1}{f_s} f_b \tag{5}$$

where R is the range of the object, c is the velocity of electromagnetic wave, T_s is the frequency sweep period, f_s is the frequency sweep bandwidth [10].

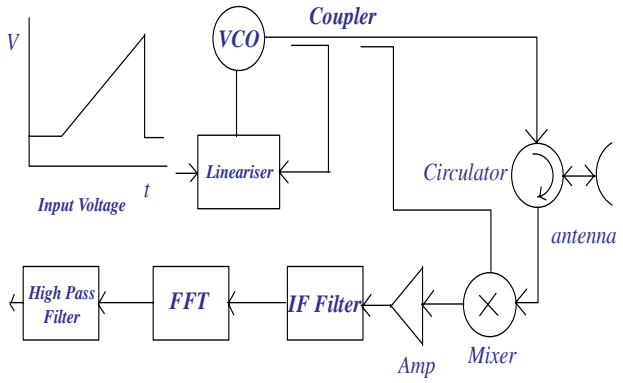

Fig. 1. Schematic block diagram of a MMW RADAR Transceiver

A. Noise in FMCW Receivers and its effect on Range Estimation

As described above, the IF filter output at the RADAR receiver can be represented by

$$v_{beat} = \frac{A_R A_T}{2}\left[\cos\left\{A_b \tau t + \left(\omega_c \tau - \frac{A_b}{2}\tau^2\right)\right\}\right] + A_R A_T\, n_R(t)\, n_T(t) \quad (6)$$

Let $\frac{A_R A_T}{2} = A^{'}$, $A_b \tau = \omega^{'}$ and $\omega_c \tau - \frac{A_b}{2}\tau^2 = \phi^{'}$ and the noise component $n(t) = A_R A_T n_R(t) n_T(t)$ Therefore the output of the IF filter can be rewritten as

$$v_{beat} = A^{'} \cos(\omega^{'} t + \phi^{'}) + n(t) \quad (7)$$

The noise $n(t)$ at the output of the IF amplifier is band limited white.

IV. RADAR Range Spectra Simulation

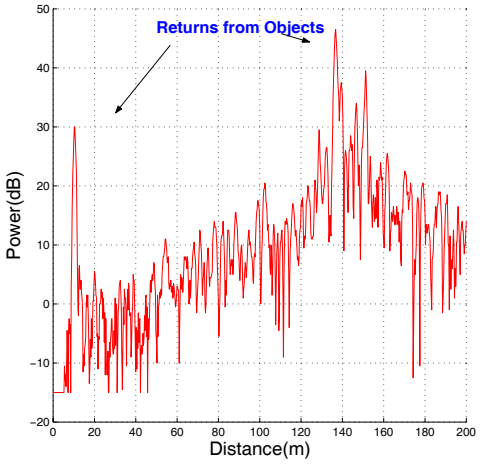

Fig. 2. Range spectrum obtained from the MMW RADAR

Figure 2 shows a single RADAR range spectra, which is the received power versus range at a constant RADAR bearing angle. As RADAR signals can penetrate through most objects, an entire range spectra at any particular bearing can be achieved. The range bin, shown in figure 2 is obtained by keeping the RADAR pointed towards a RADAR corner reflector kept arbitrarily at 10.25 metres and the second dominant reflection occurs from a building which is 138 metres from the RADAR. *i.e.* the RADAR waves are reflected from, but also penetrate the corner reflector. The corner reflector is of known RCS and can give good reflections (high signal power) back to the RADAR. The spectrum has two main features; the signal return from targets and noise. As shown in figure 2, signals are riding over a low frequency signal which increases its amplitude up to a certain range (approx. 150 metres) and decreases towards the maximum range (approx. 200 metres). This is due to the effect of the signal conditioning sections (filter roll-off) in the RADAR receiver. To understand the MMW RADAR range spectrum and to accurately simulate it, it is necessary to know the RADAR range equation and the noise distributions in the RADAR spectrum.

A method for simulating the RADAR range spectra is now presented. In the following, an introduction is given explaining the relationship between RADAR signal returned power and range. A detailed noise analysis during signal absence and presence is then shown. This is necessary in predicting the range bins accurately during target presence and target absence. RADAR range bins are then simulated and the results compare well with theoretical range bins.

A. RADAR Range Equation

The RADAR returned power P_r is proportional to the RADAR cross section of the object, σ and inversely proportional to the fourth power of range, R. The RADAR range equation is formally written as

$$P_r = \frac{P_t G^2 \lambda^2 \sigma}{(4\pi)^3 R^4 L} \quad (8)$$

where P_t is the RADAR transmitted power; G is the Antenna Gain; λ is the wavelength, (*i.e* 3.89 mm) and L the RADAR system losses.

A high pass filter is used to compensate for the R^4 drop in received signal power. In an FMCW RADAR, closer objects correspond to signals with low beat frequencies and far objects corresponds to high beat frequency signals. Therefore by attenuating low frequencies and amplifying high frequencies, it is possible to correct the range-based signal attenuation [10].

B. Interpretation of RADAR Noise

This section analyses the source of noise in MMW RADARs and its propagation through the various electronic stages and finally allows us to quantify the noise power in the received range spectra (seen in figure 2).

RADAR noise is the unwanted power that impedes the performance of the RADAR. For accurate simulation of range bins, characterisation of noise is important. The two main components of this are thermal noise and phase noise.

1) Thermal Noise: The principal contributor of noise at most RADAR frequencies is the thermal noise generated in the receiver electronics. The noise power is given by

$$P_N = k T_0 \beta \quad \text{watts} \quad (9)$$

where k is the Boltzmann constant, T_0 is the temperature and β is the noise bandwidth. By examining how this noise propagates through the FMCW RADAR electronics, it can be shown that the amplitude and relative phase of the output beat frequency signal (which is proportional to range) are affected by noise, but the beat frequency itself is unaffected. This means that the power in the beat frequency signal (found from the FFT of the beat frequency signal) contains noise, but the range estimate itself should be unaffected by the thermal noise. It can be shown by analysing the transition of this thermal (Gaussian) noise through the entire FMCW range estimation process, that when a target is present (strong received signal) the noise in the power-range spectrum follows

a Gaussian distribution. When no target is present (weak or no reflected signal) the distribution becomes Gumbel (minimum) distribution.

Measurements with target presence/absence were made to verify these distributions (successfully) and to quantify the power variance during target presence/absence.

2) Phase Noise: The phase noise results from the VCO used in the FMCW process and broadens received power peaks and reduces the sensitivity of signal detection [5]. This introduces noise into the range estimate itself.

C. Range spectra Simulation

The tools are now complete to simulate/predict RADAR spectra. In figure 3, an object with a known RCS (10 square metres) is assumed at a distance of 11 metres. As there is signal attenuation due to target range, a high pass filter is used for signal attenuation compensation. A high pass filter of gain 60 dB/decade is used. The simulated result is as shown in figure 3 (lower graph) which approximately matches the original RADAR spectrum, for the real target shown in figure 4.

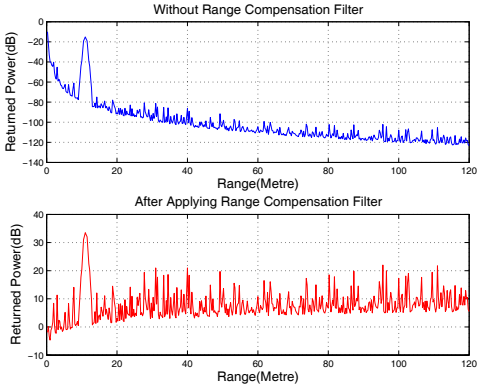

Fig. 3. Simulated RADAR Spectrum. The first figure shows the range spectra without range compensation. The second figure shows the effect of the range compensation (high pass) filter.

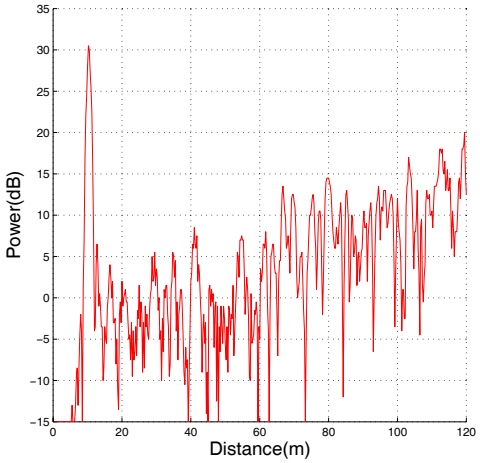

Fig. 4. Power vs. range of a single range bin obtained from a RADAR scan.

A method for realistically predicting the RADAR range spectra has been shown here which can be used for predicting observations within a SLAM framework.

V. Feature Detection based on Target Presence Probability

To try and "pick-out" the true range values from range bins, previous methods have used a power threshold on the range bins (the first power to exceed some threshold gives the closest object) [2] or Constant False Alarm Rate techniques (CFAR) [11] [9]. The problem with the thresholding method is, it requires human interpretation/intervention for adjusting the threshold. CFAR method tends to work well with aircraft in the air having relatively large RCS, while surrounded by air (with extremely low RCS). At ground level however, the RCS of objects is comparatively low and also there will be clutter (objects which cannot be reliably extracted). The CFAR can then misclassify features as noise and noise as features. Figure 5 shows the pitfalls of the CFAR technique when applied to a range spectra obtained when the environment contains only two objects downstream approximately 128 metres apart. The circles indicate the detection of target. The moving average will set the threshold which will detect the target presence. As the CFAR is a binary detection technique, the output is either a one or a zero; *i.e.* either target presence or target absence. The combination of subsequent observations is more difficult with this discrete representation. The problem arises when the technique classifies noise as signal.

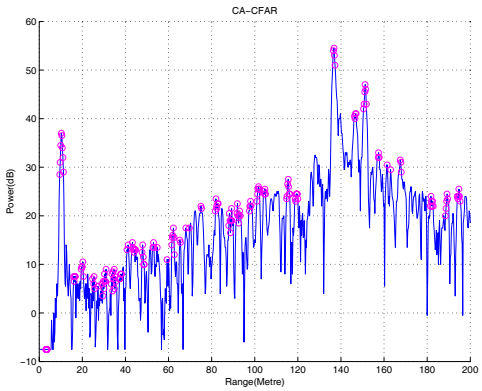

Fig. 5. The graph shows the detection of features using a CFAR threshold. CFAR misclassifies clutter as targets.

For typical outdoor environments, the RADAR cross section of objects may be small. The smaller returned power from these objects can be buried in noise. For extracting these smaller signal returns, a method is now introduced which uses the probability of target presence [12] for feature detection. The detection problem described here can be stated formally as a binary hypothesis testing problem [13]. The feature detection can be achieved by estimating the noise power contained in the range spectra. The noise estimate is performed by averaging past spectral power values and using a smoothing parameter. This smoothing parameter is adjusted by the target presence

probability in the range bins. The target presence probability is obtained by taking the ratio between the local power of range spectra containing noise and its minimum. The noise power thus estimated is then subtracted from the range bins to give a reduced noise range spectra.

Let the power of the noisy range spectra be smoothed by a w-point window function $b(i)$ whose length is $2w+1$

$$\check{P}(k,l) = \sum_{i=-w}^{w} b(i)\,\check{P}(k-i,l) \tag{10}$$

where $\check{P}(k,l)$ is the k-th power value of l-th range spectra.

Smoothing is then performed by a first order recursive averaging technique:

$$\check{P}(k,l) = \alpha_s \check{P}(k,l-1) + (1-\alpha_s)\,\check{P}(k,l) \tag{11}$$

where $\alpha_s\,(0 < \alpha_s < 1)$ is a weighting parameter. First the minimum and temporary value of the local power is initialised to $P_{min}(k,0) = P_{tmp}(k,0) = \check{P}(k,0)$. Then a range bin wise comparison is performed with the present bin l and the previous bin $l-1$.

$$P_{min}(k,l) = \min\{P_{min}(k,l-1),\,\check{P}(k,l)\} \tag{12}$$
$$P_{tmp}(k,l) = \min\{P_{tmp}(k,l-1),\,\check{P}(k,l)\} \tag{13}$$

When L range bins have been read, the temporary variable, P_{tmp} is initialised by

$$P_{min}(k,l) = \min\{P_{tmp}(k,l-1),\,\check{P}(k,l)\} \tag{14}$$
$$P_{tmp}(k,l) = \check{P}(k,l) \tag{15}$$

Let the signal-to-noise power, $\mathrm{P}_{SNP}(k,l) = \frac{\check{P}(k,l)}{\mathrm{P}_{min}(k,l)}$ be the ratio between the local noisy power value and its derived minimum.

In the Neyman-Pearson test [14], the optimal decision(*i.e.* whether target is present or absent) is made by minimising the probability of the type II error, subject to a maximum probability of type I error is as follows.

The test, based on the *likelihood ratio*, is

$$\frac{p(\mathrm{P}_{SNP}\,|\,\mathrm{H}_1)}{p(\mathrm{P}_{SNP}\,|\,\mathrm{H}_0)} \underset{\mathrm{H}_0}{\overset{\mathrm{H}_1}{\gtrless}} \delta \tag{16}$$

where δ is a threshold; H_0 and H_1 designate hypothetical target absence and presence respectively. $p(\mathrm{P}_{SNP}\,|\,\mathrm{H}_0)$ and $p(\mathrm{P}_{SNP}\,|\,\mathrm{H}_1)$ are the conditional probability density functions. The decision rule of equation 16 can be expressed as

$$\mathrm{P}_{SNP}(k,l) \underset{\mathrm{H}_0}{\overset{\mathrm{H}_1}{\gtrless}} \delta \tag{17}$$

an indicator function, $\mathrm{I}(k,l)$ is defined where, $\mathrm{I}(k,l) = 1$ for $\mathrm{P}_{SNP} > \delta$ and $\mathrm{I}(k,l) = 0$ otherwise.

The estimate of the conditional target presence probability, $\hat{p}'(k,l)$ is

$$\hat{p}'(k,l) = \alpha_p \hat{p}'(k,l-1) + (1-\alpha_p)\,\mathrm{I}(k,l) \tag{18}$$

This signal presence probability can be used as a target likelihood within the SLAM formulation. $\alpha_p(0 < \alpha_p < 1)$ is a smoothing parameter. The value of α is chosen in such a way that the probability of target presence in the previous range bin has very small correlation with the next range bin.

The variance of the noise, $\hat{\lambda}'(k,l+1)$ in k-th range bin is then denoted by

$$\hat{\lambda}'(k,l+1) = \tilde{\alpha}_d(k,l)\hat{\lambda}_d(k,l) + [(1-\tilde{\alpha}_d)(k,l)]\mathrm{P}_{SNP}(k,l) \tag{19}$$

where

$$\tilde{\alpha}_d(k,l) = \alpha_d + (1-\alpha_d)p'(k,l) \tag{20}$$

Subtracting the estimated noise power from the noisy spectra will give a noise reduced range bin.

VI. Results

The results of the proposed target detection algorithm are shown in figure 6 where a RADAR noisy range bin ; the noise reduced range spectra and the corresponding target presence probability has been plotted.

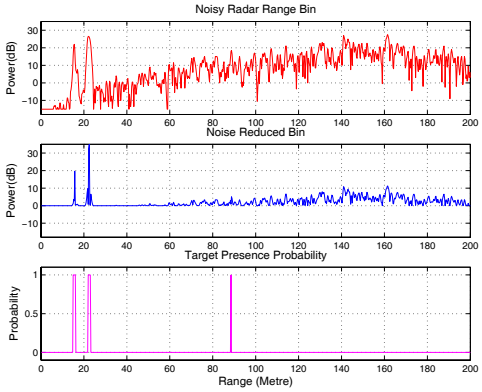

Fig. 6. Top graph: received range bin; Middle Graph: reduced noise graph; Lower Graph: probability of target presence versus range.

The target presence probability vs. range of two-dimensional RADAR scan obtained in an indoor sports hall and and outdoor scene are shown in figures 7 and 8. Figure 7 shows the target presence probability plot of an Indoor Stadium. The four walls of the stadium are clearly obtained by the proposed algorithm. Figure 8 is obtained from an outdoor field. The detected features are clearly marked in the figure. The false alarm shown in figure 8 is obtained when the RADAR beam hits the ground due the unevenness of the field surface.

The merit of the proposed algorithm is shown in figure 9 where figure shows plots obtained by different thresholds applied on RADAR range spectra and is compared with the threshold applied to the probability plot. Target presence

probability will either be a 1 or a 0. Feature detection using the target presence probability is then independent of the threshold value chosen.

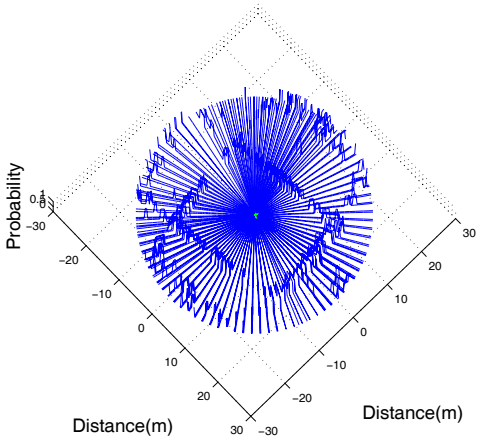

Fig. 7. Target presence probability vs. Range of a two-dimensional RADAR scan in indoor environment. The probability of the targets detected ($i.e.$ walls) are shown in the figure.

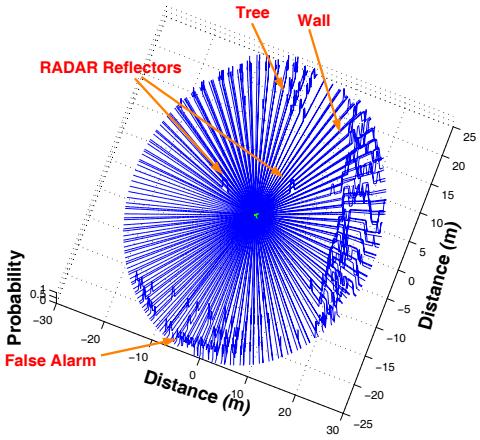

Fig. 8. Target presence probability vs. Range of a two-dimensional RADAR scan in outdoor environment. The scan is taken in a football stadium. The probability of the targets detected ($i.e.$ RADAR reflectors, wall and tree) are shown in the figure.

VII. Conclusion

This paper shows a method to accurately simulate range spectra using the RADAR range equation and a detailed noise analysis. This is very important in SLAM for generating predictions and also, providing an interpretation for observed targets. A noise distribution analysis of the RADAR range spectra was addressed. This is required for simulating the RADAR spectra realistically. Feature detection based on target presence probability is explained and it is shown that this method shows a better performance over CFAR techniques and constant threshold method in the presence of clutter. This work is a step towards building reliable maps and localising a vehicle to be used in mobile robot navigation. In future work, further methods of including the target presence probability of feature estimates into SLAM is to be investigated.

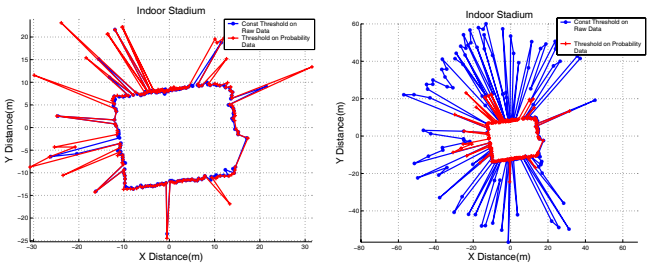

(a) A Constant threshold = $25dB$ is chosen and compared with the threshold applied on probability-range spectra.

(b) A Constant threshold = $40dB$ is chosen and compared with the threshold applied on probability-range spectra.

Fig. 9. Power vs. range and the corresponding target presence probability vs. range spectra taken from a two-dimensional RADAR scan in an indoor environment. The figures shows a comparison of the proposed feature detection algorithm with the Constant Threshold method.

VIII. Acknowledgements

This work was funded under the second author's AcRF Grant, RG 10/01, Singapore. We gratefully acknowledge help from SIMTech in the use of their utility vehicle and valuable advice from Graham Brooker (ACFR) and Steve Clark (Navtech Electronics, UK).

References

[1] scheding S, Brooker, Hennessy, Bishop, and Maclean. Terrain imaging millimetre wave radar. In *International Conference on Control, Automation, Robotics and Vision, Singapore.*, Nov. 2002.

[2] Steve Clark. *Autonomous Land Vehicle Navigation Using Millimetre Wave Radar*. PhD thesis, Australian Centre for Field Robotics, University of Sydney, 1999.

[3] Steve Clark and Hugh Durrant-Whyte. Autonomous land vehicle navigation using millimeter wave radar. In *ICRA*, pages 3697–3702, 1998.

[4] Scott Boehmke, John Bares, Edward Mutschler, and Keith Lay. A high speed 3d radar scanner for automation. In *Proceedings of ICRA '98*, volume 4, pages 2777–2782, May 1998.

[5] Alex Foessel. *Scene Modeling from Motion-Free Radar Sensing*. PhD thesis, Robotics Institute, Carnegie Mellon University, Pittsburgh, PA, January 2002.

[6] Alex Foessel, John Bares, and William Red L. Whittaker. Three-dimensional map building with mmw radar. In *Proceedings of the 3rd International Conference on Field and Service Robotics*, Helsinki, Finland, June 2001. Yleisjljenns - Painnoprssi.

[7] Hans Moravec and A. E. Elfes. High resolution maps from wide angle sonar. In *Proceedings of the 1985 IEEE International Conference on Robotics and Automation*, pages 116–121, March 1985.

[8] Sebastian Thrun. Learning occupancy grids with forward models. In *Proceedings of the Conference on Intelligent Robots and Systems*, Hawaii, 2001.

[9] M.I Scolnik. *Introduction to Radar Systems*. McGraw Hill, New York, 1982.

[10] Dirk Langer. *An Integrated MMW Radar System for Outdoor Navigation*. PhD thesis, Robotics Institute, Carnegie Mellon University, Pittsburgh, PA, January 1997.

[11] N.C Currie and C.E.Brown. *Principles and Applications of MMW Radar*. Artech House, Dedham,MA, 1987.

[12] Israel Cohen and Baruch Berdugo. Noise estimation by minima controlled recursive averaging for robust speech enhancement. In *IEEE Signal Processing Letters*, volume 9, 2002.

[13] H.L. Van Trees. *Detection, Estimation and Modulation Theory - Part I*. Willey, New York, 1968.

[14] T. Kirubarajan and Y.Bar-Shalom. *Multisensor-Multitarget Statistics in Data Fusion Handbook*. CRC Press,Boca Raton, 2001.